Δελτίο της Ελληνικής Γεωλογικής Εταιρίας τομ. XXXX, 2007
Πρακτικά 11ου Διεθνούς Συνεδρίου, Αθήνα, Μάιος 2007

Bulletin of the Geological Society of Greece vol. XXXX, 2007
Proceedings of the 11th International Congress, Athens, May, 2007

MISLOCATION VECTORS FOR THE TRIPOLI SEISMIC ARRAY, GREECE, AND STRUCTURAL EFFECT IMPLICATIONS FROM BACKAZIMUTH AND SLOWNESS RESIDUAL ANALYSIS

Pirli M.[1], Pirlis E.[1], and Voulgaris N.[1]

[1] *National and Kapodistrian University of Athens, Faculty of Geology and Geoenvironment, Department of Geophysics - Geothermics, pirli@geol.uoa.gr, epirlis@geol.uoa.gr, voulgaris@geol.uoa.gr*

Abstract

Tripoli Seismic Array, Greece, performance in terms of event location is restricted by its very small aperture and limited number of sensors. Detailed investigation of errors in automatic location results suggests structural and local geology effects. In order to investigate the possibility to correct for systematic errors automatically, mislocation vectors were calculated for an extended data-set. Theoretical values were calculated based on earthquake catalogues compiled by the National Observatory of Athens and the ISC. Resulting mislocation vectors are characterized by significant vector length, consistent with the large observed backazimuth and slowness residuals, the smaller values being met in the area NE of the array and for epicentral distance values less than 200 km. As expected, resulting corrections mostly concern backazimuth values and are not able to sufficiently affect the final epicentre solution, as the largest automatic algorithm errors are observed in epicentral distance determination. However, the possibility to automatically correct for systematic deviations is verified, and future research with an extended array configuration is expected to provide clearer results, due to significantly lower scatter.

Key words: *automatic algorithm, slowness vector, correction, dipping layer.*

Περίληψη

Η αποτελεσματικότητα της Σεισμικής Διάταξης Τριπόλεως (TRISAR) στον προσδιορισμό των εστιακών παραμέτρων των σεισμών περιορίζεται από το μικρό ανάπτυγμα και αριθμό αισθητήρων αυτής. Η λεπτομερής ανάλυση των σφαλμάτων στον αυτόματο προσδιορισμό επκέντρων δημιουργεί υπόνοιες για επιδράσεις της δομής του φλοιού και της τοπικής γεωλογίας. Για τη διερεύνηση της δυνατότητας αυτόματης διόρθωσης των αποτελεσμάτων του ανύσματος βραδύτητας, υπολογίστηκαν τα ανύσματα διόρθωσης για ένα εκτεταμένο δείγμα δεδομένων. Οι θεωρητικές τιμές προσδιορίστηκαν βάσει των σεισμικών καταλόγων του Εθνικού Αστεροσκοπείου Αθηνών και του Διεθνούς Σεισμολογικού Κέντρου (ISC). Τα ανύσματα διόρθωσης, που προέκυψαν, έχουν σημαντικό μήκος, σύμφωνο με τα μεγάλα σφάλματα που παρατηρούνται για το αζιμούθιο και τη βραδύτητα. Οι μικρότερες τιμές διαπιστώνονται ΒΑ της διάταξης, για επικεντρικές αποστάσεις μικρότερες των 200 km. Όπως είναι αναμενόμενο, οι διορθώσεις αφορούν κυρίως στο αζιμούθιο και δεν είναι αρκετές ώστε να επηρεάσουν

την τελική λύση, δεδομένου ότι τα μεγαλύτερα σφάλματα του αυτόματου αλγόριθμου αφορούν στον προσδιορισμό της επικεντρικής απόστασης. Ωστόσο, καθίσταται σαφής η δυνατότητα αυτόματης διόρθωσης του ανύσματος βραδύτητας, αναμένεται δε μία βελτιωμένη γεωμετρία της σεισμικής διάταξης να δώσει πολύ καλύτερα αποτελέσματα, κυρίως λόγω της μειωμένης διασποράς, που θα επιτυγχάνει.

Λέξεις κλειδιά: *αυτόματος αλγόριθμος, άνυσμα βραδύτητας, διόρθωση, κεκλιμμένη ασυνέχεια.*

1. Introduction

The Tripoli Seismic Array (TRISAR) was installed by the Seismological Laboratory of the University of Athens in the vicinity of the town of Tripoli, central Peloponnese, Greece, on July 16, 2003. It is a 4 element, small-aperture array of experimental character, aiming to assess array performance in terms of seismicity monitoring and earthquake location in the area of Greece. Three short-period sensors are situated at the peaks of an almost equilateral triangle with a maximum side length of approximately 250 m (Fig. 1). A broadband station, serving as reference element, is situated in the middle of this deployment (Pirli *et al.* 2004). All array elements are equipped with 3-component instruments and are installed on a plane area without elevation differences.

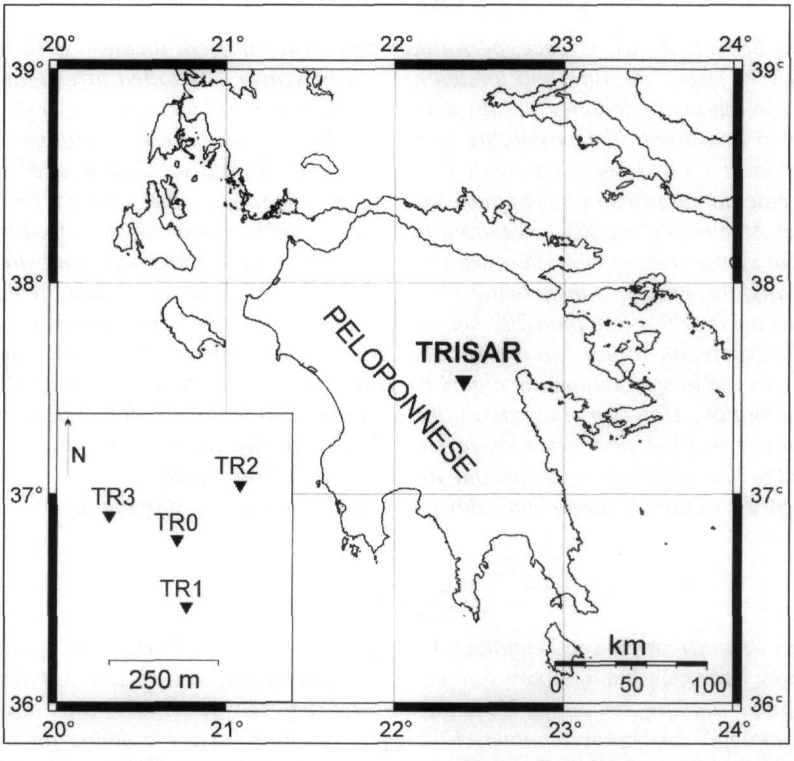

Figure 1 – Tripoli Seismic Array (TRISAR) location and configuration

Current TRISAR configuration does not support real-time data processing, so array data undergo a real-time processing simulation using the DP, EP and RONAPP algorithms (Fyen 1987, 1989, Mykkeltveit and Bungum 1984) developed at NORSAR. Automatic processing involves detection of seismic phases within array records (DP – Detector Processor), slowness vector estimation for each phase (EP – Event Processor), and individual phase grouping into seismic events (RONAPP – Regional ON-line Array Processing Package), which are then located using the TTAZLOC algorithm (Bratt and Bache 1988). Automatic algorithm results are reviewed by an analyst.

TRISAR restricted aperture and small number of sensors result in poor array resolution in terms of slowness and backazimuth estimation, consistent with the rather wide main-lobe of the transfer function for frequencies lower than 15 Hz (Pirli *et al.* 2004, Pirli 2005). Slowness distribution is characterised by very large scatter, introducing significant uncertainties in seismic phase discrimination. Backazimuth exhibits large standard deviation values, especially for epicentral distances larger than 180 km, due to very limited array aperture. Optimum epicentral distance range for TRISAR is between 40 and 180 km, slowness vector determinations being also validated by high spatial coherence levels (Pirli 2005).

Afore mentioned restrictions have a drastic effect on automatic algorithm performance. Indeed, even though automatic detector performs very satisfactorily, detecting 98% of the recorded seismicity, only a small number of the detected phases are eventually grouped into locatable events. Moreover, a significant percentage of the automatically located events are characterised by large deviations compared to true locations (Fig. 2). This is the effect of frequent phase misidentifications and wrong groupings, due to poor slowness resolution (Pirli 2005, Pirlis 2006).

In order to investigate further the distribution, size and origin of backazimuth and slowness uncertainties, mean mislocation vectors are calculated for the Tripoli Seismic Array for the automatically processed data (Schweitzer 1994, 2001). Mislocation vector estimation results are then introduced into the automatic processing procedure, so that appropriate backazimuth and slowness corrections are applied to each determined slowness vector. Corrected results are then evaluated to assess the overall automatic correction process and its contribution to earthquake location results improvement. Finally, an interpretation of backazimuth and slowness residual distribution is attempted.

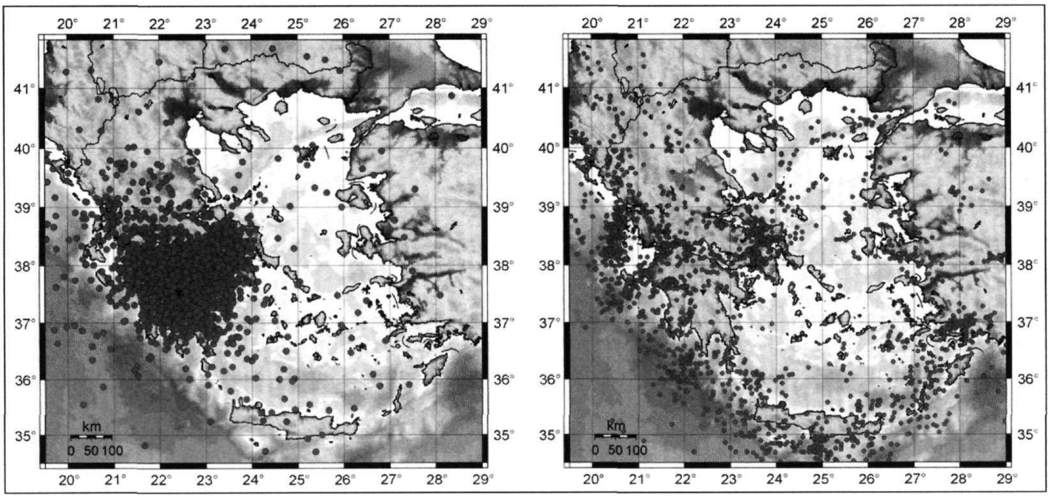

Figure 2 – Automatic algorithm epicentre location for TRISAR data within the time intervals July – August 2003, October 2003 – May 2004 and December 2004 – January 2005 (left). Seismicity in the broader area of Greece for the same time intervals located by NOA and ISC (right). TRISAR location is noted by a black, inverted triangle

2. Methodology and Data

Scatter in slowness vector determination by small-aperture arrays is usually significant and should be attributed to their restricted resolution. An additional contributor is automatic calculation of slowness parameters, as it has been observed that scatter is less for manually processed onsets. However, despite the large scatter, systematic slowness deviations have been observed at small aperture arrays (Schweitzer 1992, 2001, Harjes *et al.* 1994).

The primary aim of this research being to investigate possible systematic deviations and scatter in slowness vector estimation for TRISAR, mislocation vectors are calculated with respect to the 'observed' values (correction vectors). Owing to the large scatter characterising single observations, mean vectors are used. To achieve this, slowness-azimuth space is divided into bins, each one of them being assigned a minimum of 3 observations, in order to ascertain the validity of the results. Such a vector, $\overrightarrow{soc}$, would point from one bin of observations $\overrightarrow{so}$ to the most likely 'true' theoretical slowness $\overrightarrow{st}$, the mean correction vector for the *j*-th bin being the mean value of *n* slowness deviations in this bin (Schweitzer 2001):

Equation 1 - Formula for Correction Vectors

$$\overrightarrow{soc} = \frac{\sum_{i=1}^{n} (\overrightarrow{so_i} - \overrightarrow{st_i})}{n}.$$

Information contained in these vectors can be used to correct systematic slowness deviations and reduce scatter in the data, as attempted for the TRISAR data-set used in this research. Thereby, the automatic location process was eventually repeated, allowing for correction of backazimuth and slowness values.

In order to obtain information regarding the 'theoretical' slowness vector, a list of reference events needs to be compiled. Pairs of reference events and corresponding TRISAR onsets are identified, and epicentral distance, backazimuth, seismic phases' onset-times and expected slowness are determined for the reference list with respect to TRISAR. Both P- and S-wave phases are used. To obtain theoretical values, an appropriate velocity model for the broader area of Greece is used (Pirli 2005).

TRISAR data used for the calculation of mean mislocation vectors cover the following time intervals:

- July 26, 2003 to August 16, 2003.
- October 30, 2003 to May 19, 2004.
- December 11, 2004 to January 31, 2005.

In between the array was not in operation, as one or more elements had been experiencing technical problems, their very restricted number making it impossible to use the remaining ones for slowness vector determination.

Array data were converted to CSS3.0 database format (Anderson *et al.* 1990) in order to be compatible with the DP, EP and RONAPP automatic detection, processing and location algorithms. An STA/LTA detector run through the data, providing detections for single phases, each one of them being processed so, that the slowness vector was calculated using broadband f-k analysis (Kværna and Doornbos 1986, Kværna and Ringdal 1986). Then, single phases were grouped into events and located using the TTAZLOC algorithm, providing epicentre coordinates and local magnitude values. Event Processor generated lists containing slowness vector results were used to calculate the mean mislocation vectors.

To achieve this, as already mentioned, a list of reference events had to be used. In the case of the Tripoli Seismic Array which is mainly targeting seismicity in the area of Greece, National Observatory of Athens (www.gein.noa.gr) catalogues were used for the corresponding time intervals. In order to receive information for a wider slowness value range, the reference list was enriched with events of magnitude larger than 5.0 listed in the ISC Bulletin (ISC 2006). Thus, a reference event list containing more than 10000 entries was compiled, double entries being carefully eliminated.

To link a reference event to an event automatically detected by TRISAR, some limitations need to be applied. Thus, the onset-time residual accepts values between -10 and 10 sec, while the slowness vector residual length should not exceed a value of 10 sec/°. Once mislocation vectors are calculated, more rules need to be taken into consideration to select a number of acceptable vectors from the whole population. For this task, the onset-time residual is set to 4.0 sec for P- and 8.0 sec for S-wave phases, and maximum acceptable slowness vector length is set to 10.0 sec/° for P- and 15.0 sec/° for S-wave phases.

3. Discussion

According to the parameter settings discussed in the previous section, 252 mean mislocation vectors have been computed, the mean vector length being equal to 5.04 sec/°. Mean slowness residual is equal to 0.93 sec/° with a standard deviation of 4.49 sec/°. Residual and standard deviation values for backazimuth are -6.5° and 35.5° respectively. Overall scatter for slowness and backazimuth is equal to 4.56 sec/° and 36.1°, while the overall length of the mean mislocation vector equals 6.37 sec/°.

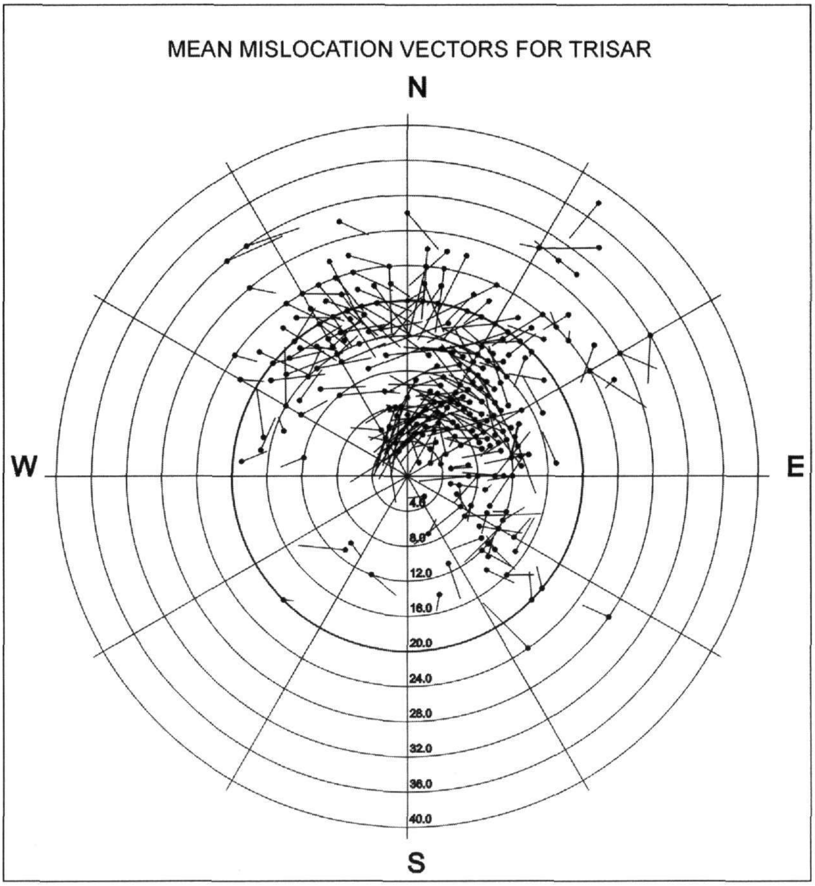

Figure 3 – Mean mislocation vectors for the Tripoli Seismic Array. Black circles denote the 'theoretical' value. The thick, black line at 20.0 sec/° is the slowness limit between P- and S-wave phases

The mean mislocation vectors for TRISAR, calculated for at least 3 observations, are plotted in Figure 3, where the 'theoretical' value is denoted by a black circle. Since both P- and S-wave phases have been used, a thick black line (20 sec/°) is used to separate theoretical slowness value for the two different phase groups.

Most of the calculated vectors are characterised by significant length, the lower values being observed at the area NE of the array, where in general TRISAR exhibits better performance (Pirli 2005, Pirlis 2006). It is difficult to discern any systematic trends either in slowness or backazimuth residual, however some more general features can be observed. Between 300° and 360° backazimuth residuals are positive, the observed value being larger than the 'theoretical'. Residual sign changes between 0° and 45°, whereas it is difficult to draw any conclusion for backazimuth values between 45° and 150°. Between 150° and 300° available data is too poor to provide any possibility of valid observation. As far as slowness residual is concerned, most values for local/regional events are positive in contrast to small slowness values that may represent phases of far-regional or teleseismic events.

A more detailed image of the backazimuth and slowness residual distribution for the data-set used to calculate the mislocation vectors for TRISAR can be obtained from Figures 4 and 5. Figure 4 provides the distribution of backazimuth residual versus 'true' backazimuth for Pn, Pg, Sn and Sg phases, while Figure 5 provides the distribution of slowness residual versus 'true' backazimuth for the same phases.

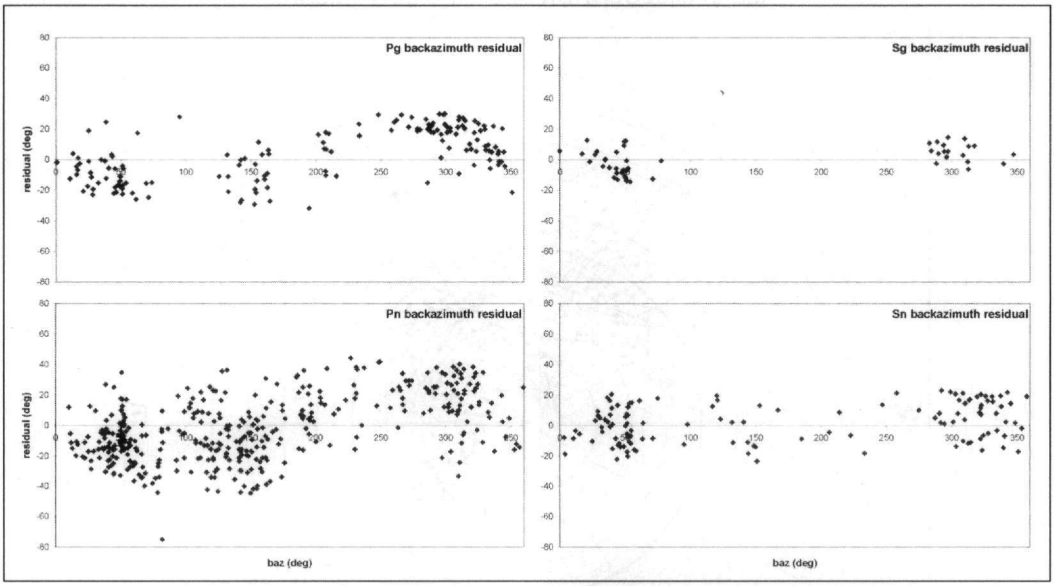

Figure 4 – Backazimuth residual distribution for Pg, Pn, Sg and Sn phases of the reference events used for mislocation vectors calculation

The large backazimuth and slowness residuals observed in Figures 4 and 5 are consistent with the large mislocation vectors length reported previously. Backazimuth residual for Pg phases is clearly lower than for Pn phases, whereas for corresponding S-wave phases used, data are too scarce to provide substantial conclusions. No similar observation can be made for the slowness residual, whose distribution is in general much more diffuse than the one for backazimuth. Such a phenomenon was expected and may be attributed to the large scatter in slowness for an array of such restricted aperture as TRISAR.

Consistent to the image obtained from Figure 3 is also the change in residual sign observed both for slowness and backazimuth, although the general trend is much more pronounced for backazimuth. The shift in residual sign takes place around backazimuth value 0° and 180°, both for Pg and Pn phases for backazimuth. Regarding slowness, this shift seems to be taking place for slightly different values, 50° and 230°, although the large scatter prevents accurate conclusions.

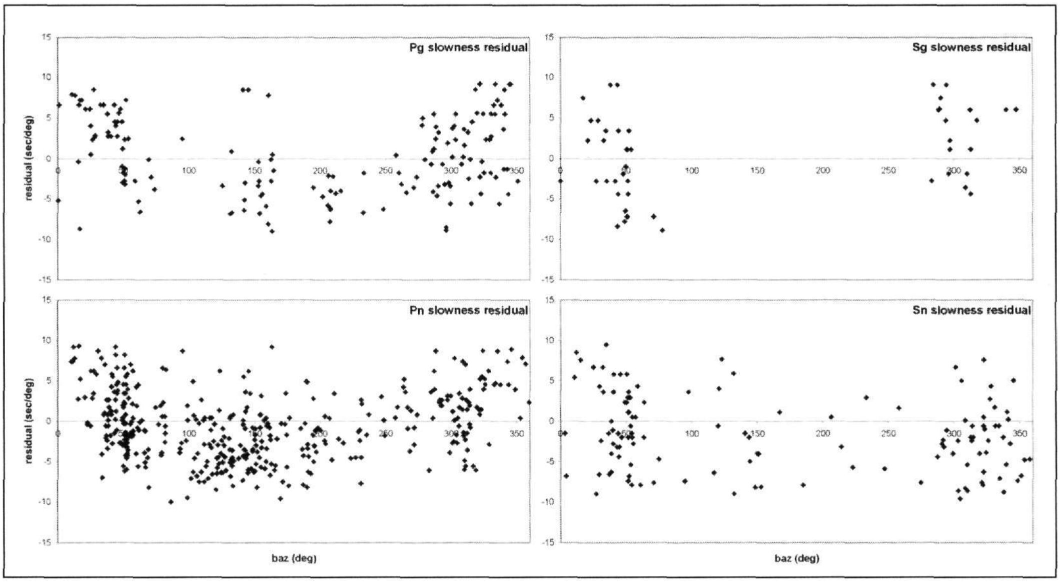

Figure 5 – Slowness residual distribution for Pg, Pn, Sg and Sn phases of the reference events used for mislocation vectors calculation

Several researchers have linked such backazimuth residual sign shifts to the effect of dipping structure underneath or in the vicinity of the recording network or array (e.g. Niazi 1966, Lin and Roecker 1996). According to Niazi (1966), the distribution of the residual and in particular the zero crossings can provide information regarding the geometry of this dipping layer. Thus, strike is determined as the midpoint between the two zero crossings and direction of dip corresponds to the zero crossing value, that if read clockwise, is the transition point from negative to positive backazimuth residual values. A rough estimate of accuracy can be expressed as the backazimuth value range for which residuals are observed both in the negative and positive value space. It is evident that with the available data within the present study, it is exceedingly difficult to obtain a valid indication of the geometry of the dipping structure affecting TRISAR data. The clearest image is that obtained for Pg phase data, which is anyhow characterised of uncertainty in the observation in the order of 50°. If we were however to attempt a quantitative approach, this would suggest a dipping layer of general E-W strike, dipping towards the South.

From extensive geophysical investigations conducted in the area where TRISAR is situated (Alexopoulos 1998), a sedimentary layer of approximately 100 m thickness is overlaying the alpine basement. Array stations are installed on this layer, which in this point has a thickness of 95 m. Such sedimentary layers have been reported to affect slowness vector estimation (e.g. Krüger and Weber 1992). However, no clear image exists at this point of the precise geometry of this layer. Moreover, previous research on overall TRISAR performance (Pirli 2005, Pirlis 2006) has indicated that there is an obvious deviation in array performance between the area East and West of TRISAR, the latter case being characterised by inferior quality results and system performance. Such an observation seems to be coinciding well with the general geological regime in the Peloponnese. The Tripoli plateau where the array is located is almost in the middle of the area (Fig. 6), in a region where a transition is observed from a more complex regime in the West to a simpler situation in the East (Mariolakos *et al.* 1985). Indeed, the western part of the Peloponnese is dominated by large-scale horst and graben systems of E-W and NNW-SSE direction, and highly seismic active faults, alpine strata formations appearing multiply folded. Eastern Peloponnese exhibits mostly inactive to moderatively active faulting of NW-SE direction and alpine formations that have suffered only one phase of tectonism, at Eocene – Early Miocene. However, before any valid interpretation can be attempted for the observed residuals, more data should be included in the data-set, while the most interesting aspect would be re-estimation of the mislocation vectors for an enhanced TRISAR configuration, involving both aperture and number of sensors extension.

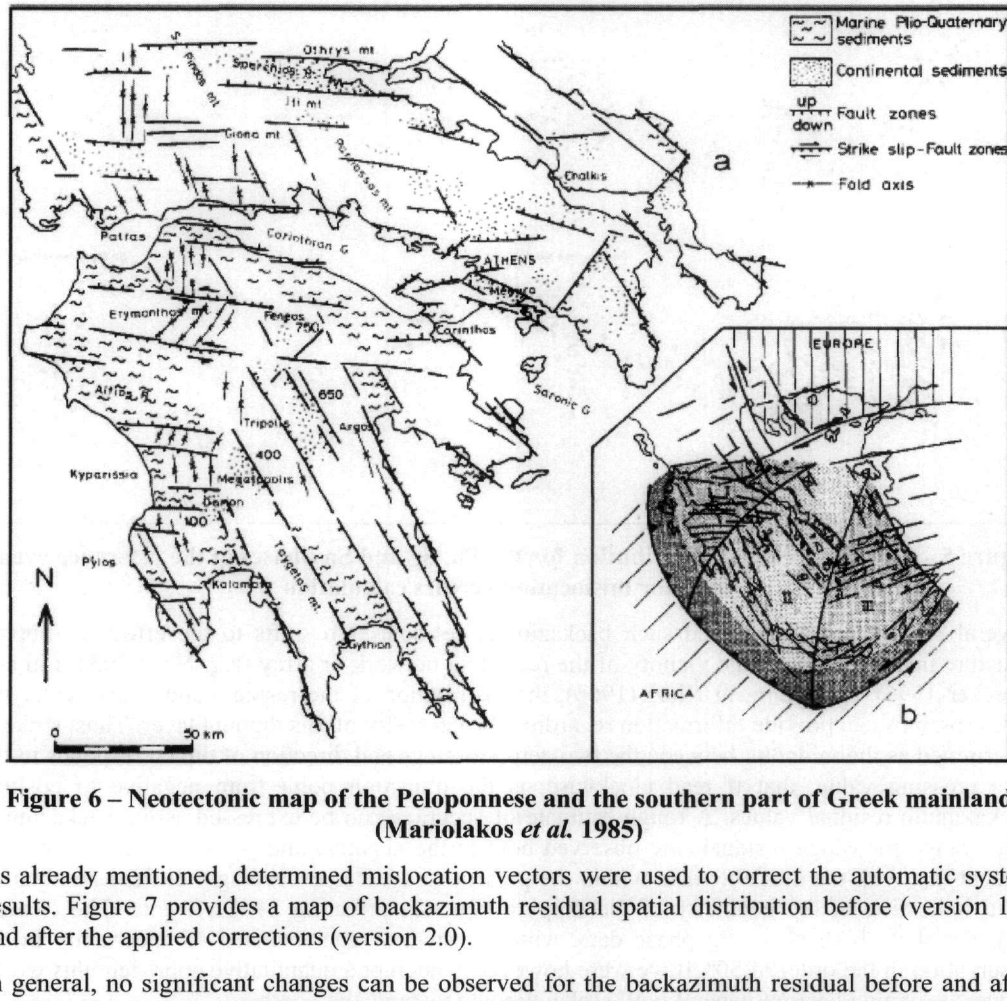

Figure 6 – Neotectonic map of the Peloponnese and the southern part of Greek mainland (Mariolakos *et al.* 1985)

As already mentioned, determined mislocation vectors were used to correct the automatic system results. Figure 7 provides a map of backazimuth residual spatial distribution before (version 1.0) and after the applied corrections (version 2.0).

In general, no significant changes can be observed for the backazimuth residual before and after the corrections were applied. A few occasional 'highs' can be observed in the corrected version, but these are restricted in large epicentral distances from TRISAR. The only area for which an enhancement is obvious is the region containing broader Attica, Evia Island and Northern Sporades Islands, indicated with a black ellipse in the lower part of Figure 7. It is interesting to point out that this is the area where TRISAR exhibits its optimum performance in slowness vector estimation and event location determination, both for automatic and manual data processing (Pirli 2005, Pirlis 2006).

In order to investigate the effect of the automatic correction procedure on epicentral distance estimation, a chart exhibiting the distribution of the epicentral distance residual against 'theoretical' distance values is presented in Figure 8. Two distributions are presented; one for the initial results (version 1.0) and one for the results after the application of calculated corrections (version 2.0). Epicentral distance values according to the solutions provided by NOA (http://www.gein.noa.gr) are used as theoretical or 'true' values.

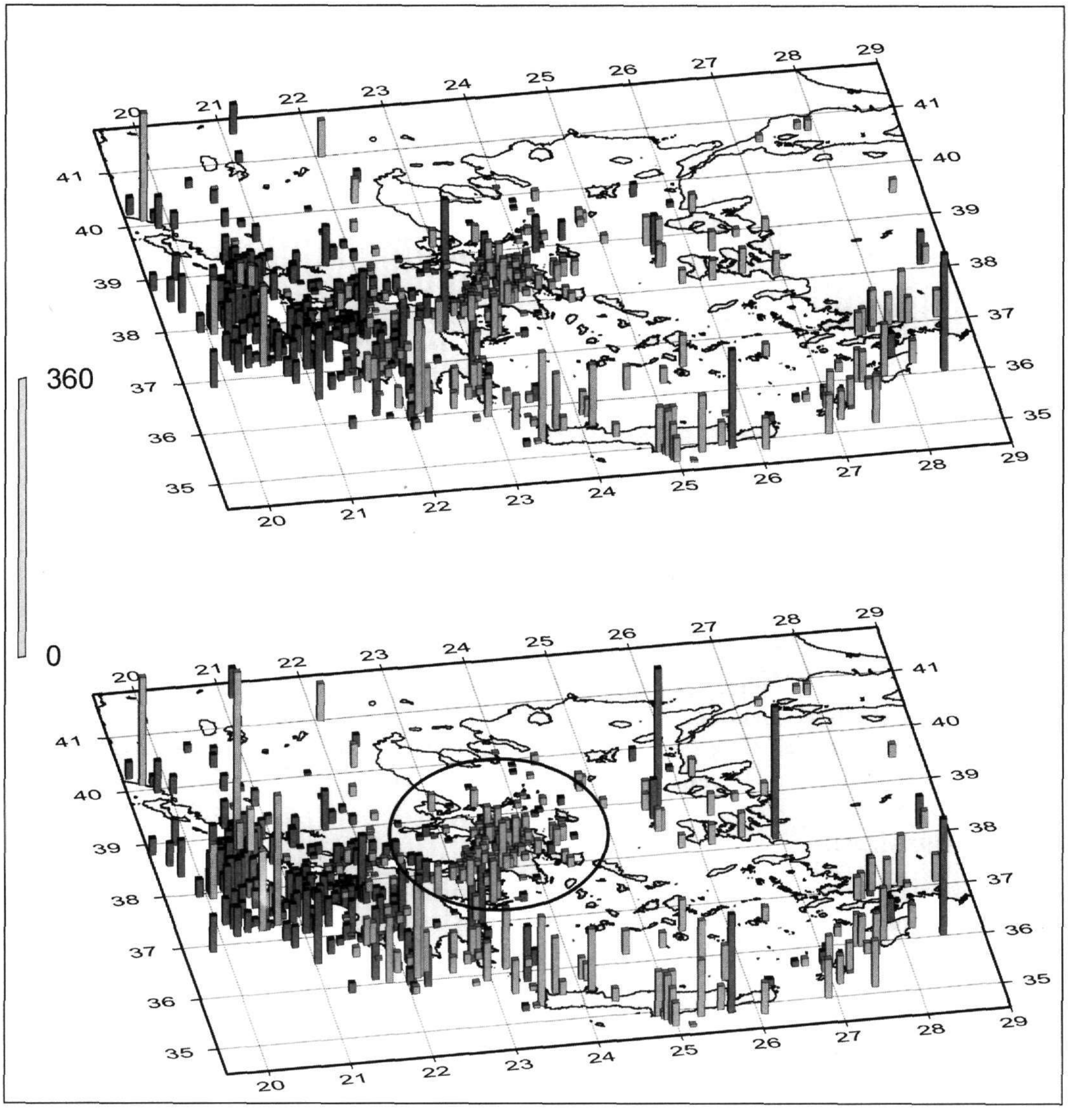

Figure 7 – Spatial distribution of backazimuth residual according to NOA locations for initial (top) and corrected (bottom) automatic algorithm results. A sub-set of common events between the two solutions is used. Residual bars are scaled from 0° to 360°, dark colour representing positive residual values and light colour negative values. The black ellipse denotes the area with the largest enhancement observed after automatic results correction

As expected, epicentral distance residual is increasing with distance. However, the image obtained from Figure 8, suggests no actual difference in residual distribution prior to and after the automatic correction was applied. The only case where a slight deviation can be observed is indicated on Figure 8 by a black ellipse, close to the distance value of 200 km. Indeed, this is the upper distance value limit for which the Tripoli array exhibits optimum performance. This slight enhancement is presumably related to corresponding improvement in backazimuth determination.

Assessing together the observations derived from backazimuth and epicentral distance residual analysis, it is quite obvious that no substantial improvements to the total of the calculated epicentre solutions can be expected. This also infers that there are only minor changes to analysed seismicity spatial distribution, compared to initial locations.

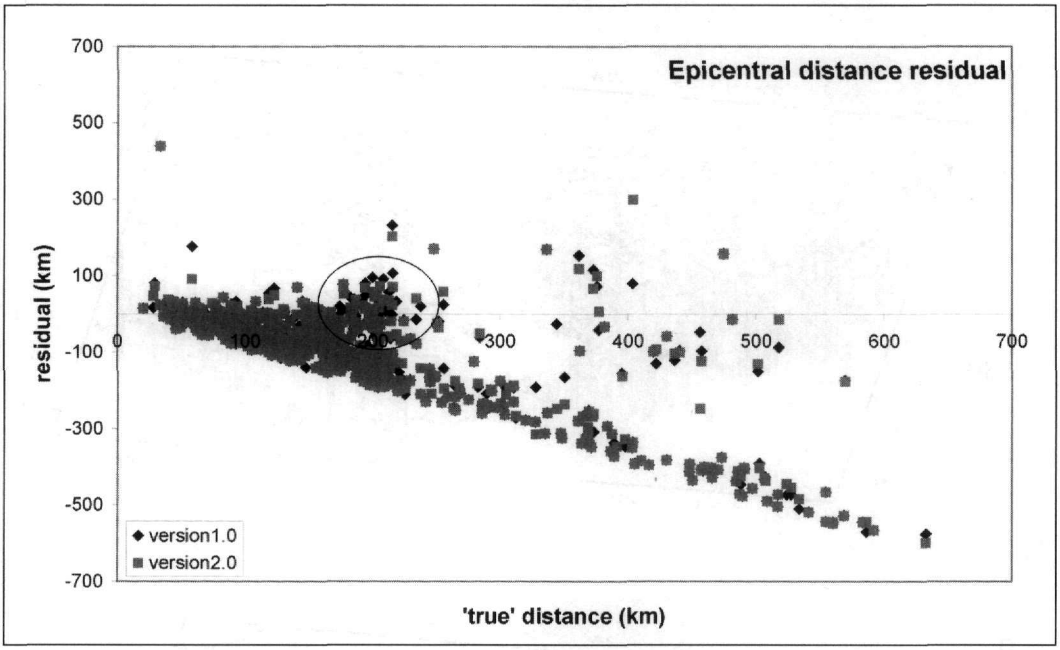

Figure 8 – Epicentral distance residual distribution for the initial (version 1.0) and corrected (version 2.0) automatic locations, according to the epicentral distance values corresponding to NOA epicentre solutions ('true' values). The black ellipse denotes the area of most significant observed enhancement.

4. Conclusions

Mean mislocation vectors were calculated for the Tripoli Seismic Array, using a data-set of earthquakes from the broader area of Greece. Resulting vectors are characterised by large length, verifying the large slowness and backazimuth residuals expected for an array of such restricted aperture and number of sensors as TRISAR. Both backazimuth and slowness residual exhibit the same general trends for the most common body-wave phases analysed by TRISAR. An even more extended data-set is expected to provide even better information on particular phase 'behaviour'.

Although intense scatter does not permit solid conclusions regarding the nature of observed deviations or on the existence of systematic anomalies, some implications regarding structural effects on backazimuth and slowness distribution are suggested. The overall residual distribution can be attributed to more than one cause, however some possible contributing factors, apart from array design and configuration, are the local geological conditions in the vicinity of the array, especially dipping layers.

Automatic correction of the results was attempted, using the information provided by the mean correction vectors calculation. In the present state, this procedure provided poor results, no actual improvement in the final epicentre solutions being observed for the vast majority of the data-set. This however has to be attributed to persisting phase misidentifications and wrong groupings made by the automatic algorithm, owing to the very poor slowness resolution of the array in its present configuration. Scheduled improvements in TRISAR configuration are expected to alter drastically its capabilities and thereby the obtained image. A similar study with the new configuration should prove very interesting in terms of verifying or disproving the interpretation of residual analysis attempted within this study.

Even under the present conditions, with only poor results obtained, the advantages and possibilities of the automatic correction procedure for the calibration of such a small-aperture array are obvious. The significance of this process is even greater under the assumption of real-time seismicity monitoring, as it can increase the validity of real- or near real-time epicentre information.

5. Acknowledgments

Research was funded within the framework of the program 'Kapodistrias' of the National and Kapodistrian University of Athens. The DP, EP and RONAPP algorithms were kindly provided by NORSAR within the framework of the ARI program (HPRI-CT-2002-00189) funded by the European Commission. Algorithms were adapted to TRISAR configuration by Johannes Schweitzer, who also provided the algorithms for mislocation vector calculation. Mary Spyridopoulou assisted in raw array data reformatting and conversion. Comments on this manuscript by Frank Krüger and an anonymous reviewer are greatly appreciated. Maps included in this paper were created using the GMT software package (Wessel and Smith 1991, 1998).

6. References

Alexopoulos, J., 1998. A contribution to the investigation of the hydrogeological regime of the Tripoli plateau, using geophysical methods, *PhD Thesis*, University of Athens, Athens, 275pp. (in Greek)

Anderson, J., Farrell, W.E., Garcia, K., Given, J., and Swanger, H., 1990. Center for Seismic Studies Version 3 Database Schema Reference Manual, *Technical Report C90-01, SAIC-90/1235*, Science Applications International Corporation, San Diego, California, 64 pp.

Bratt, S.R., and Bache, T.C., 1988. Locating events with a sparse network of regional arrays, *Bull. Seismol. Soc. Am.*, 78, 780-798.

Fyen, J., 1987. Improvements and modifications, *NORSAR Sci. Rep. 2-86/87*, NORSAR, Kjeller, Norway.

Fyen, J., 1989. Event Processor program package, *NORSAR Sci. Rep. 2-88/89*, NORSAR, Kjeller, Norway.

Harjes, H.-P., Jost, M.L., and Schweitzer, J., 1994. Preliminary calibration of candidate Alpha stations in the GSETT-3 network, *Annali Geofisica*, 37, 382-396.

ISC, 2006. *International Seismological Centre On-line Bulletin*, http://www.isc.ac.uk/Bull, Intern. Seis. Cent., Thatcham, United Kingdom.

Krüger, F., and Weber, M., 1992. The effect of low-velocity sediments on the mislocation vectors of the GRF array, *Geophys. J. Int.*, 108, 387-393.

Kværna, T., and Doorbos, D.J., 1986. An integrated approach to slowness analysis with arrays and three-component stations, *NORSAR Sci. Rep. 2-85/86*, NORSAR, Kjeller, Norway, 60-69.

Kværna, T., and Ringdal, F., 1986. Stability of various f-k estimation techniques, *NORSAR Sci. Rep. 1-86/87*, NORSAR, Kjeller, Norway, 29-40.

Lin, C.-H., and Roecker, S.W., 1996. P-wave backazimuth anomalies observed by a small-aperture array at Pinyon Flat, Southern California: Implications for structure and source location, *Bull. Seismol. Soc. Am.*, 86(2), 470-476.

Mariolakos, I., Papanikolaou, D., and Lagios, E., 1985. A neotectonic geodynamic model of Peloponnesus based on morphotectonics, repeated gravity measurements and seismicity, *Geol. Jb.*, b50, 3-17.

Mykkeltveit, S., and Bungum, H., 1984. Processing of regional seismic events using data from small-aperture arrays, *Bull. Seismol. Soc. Am.*, 74, 2313-2333.

Niazi, M., 1966. Corrections to apparent azimuths and travel-time residuals for a dipping Mohorovicic discontinuity, *Bull. Seismol. Soc. Am.*, 56, 491-509.

Pirli, M., 2005. A contribution to earthquake location in Greece with the use of seismic arrays, *PhD Thesis*, University of Athens, Athens, 256 pp. (in Greek)

Pirli, M., Voulgaris, N., Alexopoulos, J., and Makropoulos, K., 2004. Installation and preliminary results from a small aperture seismic array in Tripoli, Greece, *Bull. Geol. Soc. Greece*, XXXVI, 1499-1508.

Pirlis, E., 2006. *Evaluation of the automatic data processing algorithm and investigation of calibation possibilities for the Tripoli Seismic Array*, MSc Thesis, University of Athens, Athens, 197 pp. (in Greek)

Schweitzer, J., 1992. The GERESS contribution to the GSETT-2 experiment 1991. In *Advanced Waveform Research Methods for GERESS Recordings*, DARPA Ann. Rep. No. AFOSR-90-0189 Sci. Rep. No. 2, PL-TR-92-2142, ADA,253686, 25-49.

Schweitzer, J., 1994. Mislocation vectors for small aperture arrays – A first step towards calibrating GSETT-3 stations, *NORSAR Sci. Rep. 1-94/95*, NORSAR, Kjeller, Norway, 104-118.

Schweitzer, J., 2001. Slowness corrections – One way to improve IDC products, *PAGEOPH*, 158, 375-396.

Wessel. P. and Smith, W.H.F., 1991. Free software helps map and display data, *EOS Trans. Am. Geophys. Union*, 72, 441, 445-446.

Wessel, P. and Smith, W.H.F., 1998. New, improved version of Generic Mapping Tools released, *EOS Trans. Am. Geophys.Union*, 79, 579.